

On the Structure and Volumetric Properties of Solvated Lanthanoid(III) Ions in Amide Solutions

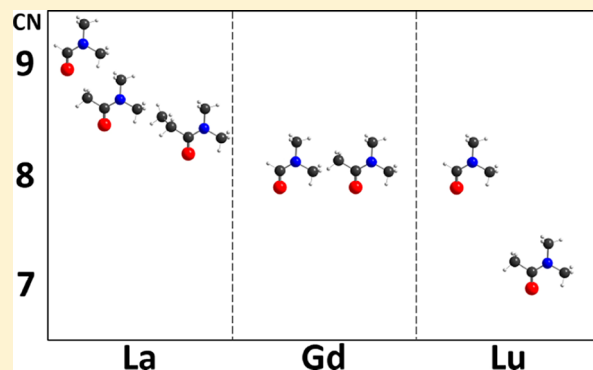
Anna Fuchs,^{†,§} Daniel Lundberg,^{†,*} Dorota Warmińska,[‡] and Ingmar Persson[†]

[†]Department of Chemistry, Swedish University of Agricultural Sciences, P.O. Box 7015, SE-750 07 Uppsala, Sweden

[‡]Department of Physical Chemistry, Chemical Faculty, Gdańsk University of Technology, ul. Narutowicza 11/12, 80-233 Gdańsk, Poland

Supporting Information

ABSTRACT: The coordination chemistry and the volumetric properties of three representative lanthanoid(III) ions—lanthanum(III), gadolinium(III), and lutetium(III)—have been studied in three amide solvents with gradually increasing spatial demand upon coordination: *N,N*-dimethylformamide (dmf) < *N,N*-dimethylacetamide (dma) < *N,N*-dimethylpropionamide (dmp). Large angle X-ray scattering (LAXS) and EXAFS have been used to determine the structure of the solvated lanthanoid(III) ions in solution, further supplemented with a crystallographic study on octakis(*N,N*-dimethylacetamide)lanthanum(III) triflate, [La(dma)₈](CF₃SO₃)₃. The selection of ions and solvents allows an estimate of the steric congestion effects on the resulting coordination number, CN, ranging from nine for lanthanum(III) ions in dmf to seven for the smaller lutetium(III) ion in space-demanding dma. The standard partial molar volumes of the solvated lanthanoid(III) ions in water and dmf are reflected in the CNs, as these solvent molecules are small enough to not interfere with each other upon coordination. However, the larger and more space-demanding dma displays a different pattern with an almost constant standard partial molar volume and a decreasing CN, counterbalancing the difference in ionic radius of the lanthanoid(III) ion.



INTRODUCTION

The lanthanoid(III) ions have been the subject of many coordination chemistry studies because of their similar physicochemical properties and incrementally decreasing ionic radii along the series. Current approaches typically focus on either structural or physicochemical properties, thereby only studying one aspect of their chemical behavior. In contrast, a dual assessment that uses both experimental categories may prove more informative, as different properties are investigated simultaneously.

The coordination chemistry approach includes studies of the structures of the hydrated, and the dimethylsulfoxide (dmsO) and *N,N'*-dimethylpropyleneurea (dmpu) solvated lanthanoid(III) ions in solid state and solution.^{1–9} These studies showed that the steric requirements of the solvent molecule will result in different coordination numbers, CNs. The hydrates all have tricapped trigonal prismatic configuration even though the heavier lanthanoid(III) ions display some water deficiency in the capping positions starting at holmium.^{1–7} The dmsO solvates are all eight-coordinate in square antiprismatic fashion,^{8,9} while all dmpu solvates except lutetium(III) are seven-coordinate in solution and six-coordinate with octahedral geometry in the solid state.^{5,6} The observed bond distances in these hydrates and solvates, together with available literature data, resulted in both new and revised ionic radii of the lanthanoid(III) ions for $6 \leq \text{CN} \leq 9$.⁵ These radii will be used

here as they were shown to be more appropriate than those reported by Shannon.¹⁰

For a study on the steric effects of ligands, the lanthanoid(III) ions are suitable as they form mainly electrostatic interactions and CNs thus become highly dependent on size of the donor atom and possible spatial demands of the backbone of the ligand. The amide solvents *N,N*-dimethylformamide (dmf), *N,N*-dimethylacetamide (dma) and *N,N*-dimethylpropionamide (dmp) feature a slight increase in size and steric requirements of their backbone structure, Figure 1. They are all aprotic, neutral solvents with very similar electron-pair donor ability, $D_s = 24$ for dmf and dma,¹¹ with a value for dmp likely in the same range though yet to be determined. Some studies have indicated that the *staggered* conformer of dmp is more favorable upon coordination than its planar *cis* equivalent.^{12–14} Combined, the lanthanoid(III) ions and these amide solvents make good model systems for a study on ligand size and steric congestion. Some of the physicochemical properties of the studied amide solvents are reported in a recent review of the area,^{15,16} and selected examples are listed in Table S1, Supporting Information.

Received: October 12, 2012

Revised: June 14, 2013

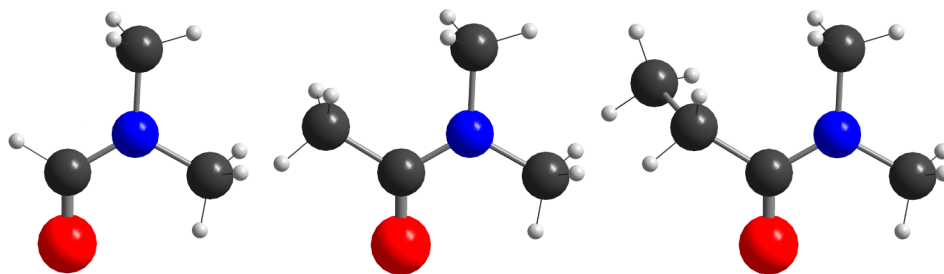


Figure 1. Structural models of the three studied amides (from left to right): *N,N*-dimethylformamide (dmf), *N,N*-dimethylacetamide (dma), and *N,N*-dimethylpropionamide (dmp, staggered).

It can be assumed that changes in coordination affect other physicochemical properties such as the partial standard molar volume. The apparent molar volume, V_{Φ} , is defined as the difference between the volume of solution and the volume of solvent calculated per mole of solute. Values depend on concentration and temperature and, by definition, their limiting values as the concentration approaches indefinite dilution are referred to as the standard partial molar volumes, V° . It is expected that V° is dependent on the coordination chemistry of the metal solvate, though not yet proven. In order to assign contributions from the cation and the anion in a completely dissociated salt, an extra-thermodynamic assumption based on the additivity rule must be applied.¹⁷ The ionic contributions can then provide information on the structure-making and structure-breaking properties of the ions depending on the sign of the value of V° . This subject has recently been reviewed for aqueous solutions by Marcus.¹⁸ In general, most metal cations, and especially high-valent ones, are structure-making, thus having the ability to compress the solvent molecules in the solvation shells in comparison to the free solvent giving negative V° values.^{18,19} In other words, they tend to organize the structure of solvent molecules in a tighter way in the proximity to the cation than in the neat solvent. In analogy with this most anions bind solvent molecules weakly due to their low charge density giving them structure-breaking properties with a positive V° value, including dmf and dma solutions.^{19,20} To better understand this phenomenon, it is convenient to present the standard partial molar volume as a sum of two contributions, the intrinsic volume and the electrostriction volume. The intrinsic volume is proportional to the cube of the ionic radius, r , whereas the electrostriction volume is proportional to the square of the ion charge, z , and inversely proportional to r , as originally proposed by Hepler:²¹

$$V^{\circ} = \frac{Ar^3 - Bz^2}{r} \quad (1)$$

where A is proportional to the size of an ion as it depends on the packing effects of the ions in the solution, while B is a solvent-dependent value.^{21,22} More sophisticated equations have been proposed in an attempt to explain the contributions to the partial molar volumes of ions in both aqueous and nonaqueous solutions. However, the original Hepler equation, with clearly defined contributions, is sufficient for our discussion. Studies concerning the thermodynamic properties of the lanthanoid(III) systems are too few for a broader discussion, whether qualitative or quantitative, as the available data almost exclusively covers aqueous solutions.^{23–28} The only nonaqueous O -donor solvent data sets reported so far are some principal thermodynamic information for lanthanoid(III)

triflate in dmf ($\text{Ln} = \text{La}$),²⁰ dmso ($\text{Ln} = \text{La}, \text{Gd}, \text{Lu}$),²⁹ and methanol ($\text{Ln} = \text{La}, \text{Gd}, \text{Lu}$).³⁰

In contrast, several structural studies of amide solvated lanthanoid(III) ions in solution have been published by Ishiguro et al.^{31–36} In one of their reviews, they report the $\text{Ln}-\text{O}$ bond distances as well as the CNs obtained by EXAFS in aqueous, dmf and dma solution.³² However, the CN parameter was refined simultaneously with the strongly correlated Debye–Waller coefficient, thereby increasing the uncertainty of both parameters. Also, the possibility to correlate CNs with bond distances from crystallographic data was not explored. Furthermore, in a series of experiments in dmf/dma mixtures, Ishiguro et al. have also been studying complex formation in bromide and chloride systems using Raman spectroscopy, where the preferential CN of the lanthanoid(III) ions was determined.^{32,33} Ultimately, they conclude that eight is the primary CN for these systems, although their own reported values differ from $\text{CN} = 8$.^{31,37} Studies on the dynamics and exchange mechanisms of solvated lanthanoid(III) ions in amide solvents have been investigated using NMR spectroscopy.^{38–42} The CN for the dmf solvated thulium(III) and ytterbium(III) ions was determined to 7.7 ± 0.2 and 7.8 ± 0.2 , respectively.^{39,40} The dmf solvated cerium(III), praseodymium(III), and neodymium(III) ions are nine-coordinate at low temperatures, and gradually convert into eight-coordinate species reaching a midpoint at 253, 235, and 215 K, respectively, while, starting at terbium(III), eight is the only observed CN.⁴¹ More recently, a variable temperature ^{17}O NMR study reports that the CN of dmf solvated gadolinium(III) ion decreases from eight at 223 K to as low as four at 373 K.⁴²

Lastly, several crystal structures containing homoleptic lanthanoid(III)/noncyclic amide complexes have been reported with $6 \leq \text{CN} \leq 9$. A thorough overview of these is given in Table S2, Supporting Information, which, for matters of completeness, also includes mixed hydrate/amide solvate complexes. The only reported crystal structure to date containing a homoleptic dma lanthanoid(III) solvate is hexakis(*N,N*-dimethylacetamide)ytterbium(III) phosphotungstate.⁴³ Solid perchlorate salts containing homoleptic dma solvated lanthanoid(III) ions have, however, been studied by IR spectroscopy and powder diffraction, where $\text{CN} = 8$ for $\text{Ln} = \text{La}-\text{Nd}$, $\text{CN} = 7$ for $\text{Ln} = \text{Sm}-\text{Er}$, and $\text{CN} = 6$ for $\text{Ln} = \text{Tm}-\text{Lu}$ were proposed.⁴⁴

The aim of this study is to present and discuss the structure of dmf, dma and dmp solvated lanthanum(III), gadolinium(III) and lutetium(III) ions in solution together with their recently reported standard partial molar volumes, V° , obtained from volumetric measurements,⁴⁵ in an attempt to reveal any relationship between volumetric properties and the coordina-

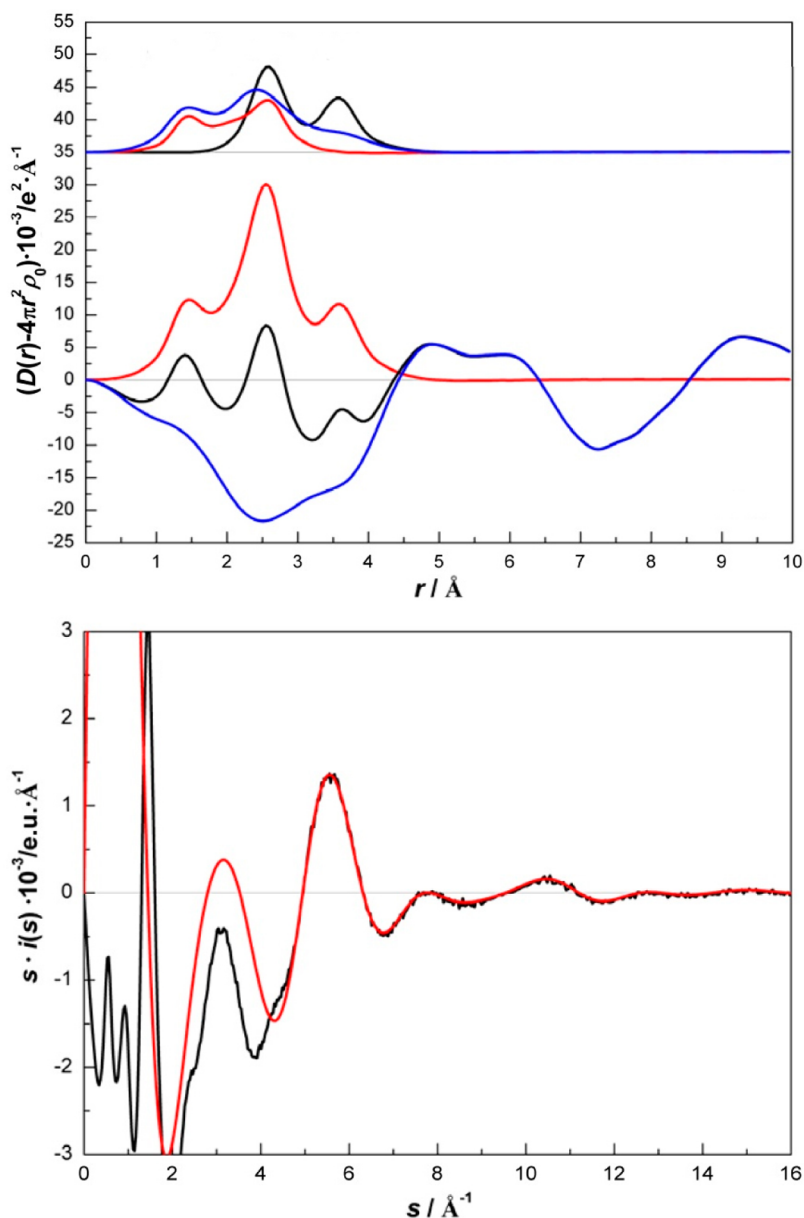


Figure 2. LAXS radial distribution function (RDF) of $\text{La}(\text{CF}_3\text{SO}_3)_3$ solution in dmf. (Top, upper pane) Separate model contributions (offset: 35) of lanthanum(III) ion solvated by dmf (black line), triflate ion (red line) and dmf solvent (blue line). (Top, lower pane) Experimental RDF (black line); sum of model contributions (red line); the difference (blue line). (Bottom) Reduced intensity function (experimental results, black line; model, red line).

tion chemistry of the solvates. The structure determination in solution was performed by combining LAXS and EXAFS measurements. To further support the data analysis of the structures in solution, the crystal structure of octakis(dma)-lanthanum(III) triflate was determined, the second homoleptic dma solvate of a lanthanoid(III) ion ever reported.

EXPERIMENTAL SECTION

Chemicals. Anhydrous lanthanum(III), gadolinium(III) and lutetium(III) triflates were prepared by dissolution of the respective oxide (Sigma Aldrich and Kebo, analytical grade, 99.9% metal basis) in aqueous slurries with triflic acid (Fluka, AR grade, $\geq 99\%$). The excess water and acid were boiled off, and the formed solid salts were mortared and dried repeatedly, and finally stored in an oven at 470 K.

Solvents. *N,N*-Dimethylformamide, dmf, (Sigma-Aldrich, AR, 99.8%) and *N,N*-dimethylacetamide, dma, (Sigma-Aldrich, ReagentPlus, $\geq 99\%$) were used without further purification. *N,N*-Dimethylpropionamide, dmp (Sigma-Aldrich, AR, 98%) was distilled under reduced pressure using calcium hydride (Merck) as a drying agent prior to use.

Solutions. The dmf, dma, and dmp solutions of the lanthanoid(III) triflates were prepared by weighing in appropriate amounts of the respective anhydrous triflate salts and dissolving them in the respective solvent. The compositions together with solution densities and absorption coefficients are given in Table S3, Supporting Information.

Large Angle X-ray Scattering Measurements. The scattering of Mo- $K\alpha$ radiation ($\lambda = 0.7107 \text{ \AA}$) on the free surface of dmf and dma solutions of lanthanum(III), gadolinium(III) and lutetium(III) triflate solutions was

measured with a large-angle θ – θ diffractometer described elsewhere.^{46,47} A polytetrafluoroethylene (PTFE) cup with solution was placed inside the radiation shield with beryllium windows. The intensity of the scattered radiation after monochromatization with a focusing lithium fluoride crystal, was measured at 450 discrete points in the range $1 < \theta < 65^\circ$; scattering angle = 2θ . A total of 100 000 counts was collected at each angle and the whole angular range was scanned twice, which corresponds to a statistical uncertainty of about 0.3%. The divergence of the primary X-ray beam was limited by 1° or $1/4^\circ$ slits for different θ regions with some parts of data overlapping for scaling purposes.

All data treatment was carried out by using the KURVLR program⁴⁸ as described in detail previously.⁴⁹ The experimental intensities were normalized to a stoichiometric unit of volume containing one metal atom, using scattering factors f for neutral atoms, anomalous dispersion correction, $\Delta f'$ and $\Delta f''$,⁵⁰ and values for Compton scattering.⁵¹ Fourier back-transformation was applied to eliminate spurious peaks not related to any interatomic distances peaks below 1.2 Å in the radial distribution function, RDF.⁵² Least-squares refinements of the model parameters were performed by means of the STEPLR program⁵³ to minimize the error square sum U :

$$U = \sum w(s) \cdot (i_{\text{exp}}(s) - i_{\text{cal}}(s))^2 \quad (2)$$

EXAFS Measurements. The EXAFS measurements at the lanthanoids' L_{III} edges were performed at Stanford Synchrotron Radiation Lightsource (SSRL), Stanford, USA, beamline 4–3, and at MAX-lab, Lund University, Sweden, beamline I811. Data collection was performed simultaneously in transmission and fluorescence mode using ion chambers with flowing nitrogen and a 13-element germanium array detector at SSRL, and ion chambers with stationary gas mixtures and either a passivated implanted planar silicon (PIPS) detector or a single element Radiant Technology Vortex silicon drift detector at MAX-lab. The EXAFS stations were equipped with Si[111] double crystal monochromators. SSRL operated at 3.0 GeV and a maximum current of 97–100 mA (top-up mode), and MAX-lab at 1.5 GeV and a maximum current of 200 mA.

In order to remove higher order harmonics, the beam intensity was detuned to 35–50% of the maximum intensity at the end of the scans for the L_{III} edge at MAX-lab, while mirrors were used at SSRL. The energy scales of the X-ray absorption spectra were calibrated by assigning the first inflection point of the L_{III} edges of reference lanthanum, gadolinium and lutetium foils to 5483, 7243, and 9244 eV, respectively.⁵⁴ For each sample, 3–4 scans were averaged, giving a satisfactory signal-to-noise ratio. Solutions were contained in cells made of 6 μm polypropylene X-ray film as windows and a PTFE spacer of appropriate thickness placed between titanium plates.

EXAFS Data Analysis. The EXAFSPAK program package⁵⁵ was used for the data treatment. The standard deviations given for the refined parameters are obtained from k^3 -weighted least-squares refinements of the EXAFS function $\chi(k)$, and do not include systematic errors of the measurements. These statistical error estimates provide a measure of the precision of the results and allow reasonable comparisons, for example, of the significance of relative shifts in the distances. However, the variations in the refined parameters, including the shift of the E_0 value (for which $k = 0$), using different models and data ranges, indicate that the absolute accuracy of the distances given for the separate complexes is within ± 0.005 to 0.02 Å for well-defined

interactions. The “standard deviations” given in the text have been increased accordingly to include estimated additional effects of systematic errors.

Single Crystal X-ray Diffraction. After many months of storing the prepared solutions in a refrigerator, a solid formed in the dma solution containing lanthanum(III) triflate, 1. Crystals were taken out of the mother liquid, mounted on thin glass capillaries, and placed under cool conditions. Data acquisition was performed on an Oxford Diffraction Xcalibur 2 cooling the crystal to 93 K. The structures were solved by the direct methods in SHELX⁵⁶ and refined using full-matrix least-squares on F^2 . Except for the disordered atoms, all non-hydrogen atoms were treated anisotropically. The methyl hydrogen atoms were calculated in ideal positions riding on their respective carbon atom. Absorption correction was applied using overlapping multiscans. The atomic coordinates, bond distances and angles are available in the Crystallographic Information File in the online Supporting Information section, with selected crystallographic information in Table S4.

RESULTS

LAXS. The radial distribution function (RDF) with the individual contributions and the corresponding intensity function for the dmf solution of lanthanum(III) triflate in dmf is given in Figure 2. The RDFs and reduced intensity functions from the LAXS experiments on the remaining dmf and dma solutions are given in Figures S1–S5, Supporting Information. All RDFs reveal three peaks at around 1.5, 2.3–2.5 and 3.5 Å, respectively. The peak at 1.5 Å corresponds to intramolecular distances in the solvent and the triflate ion. The peaks in the range 2.3–2.5 Å correspond to the Ln–O bond distances of the dmf and dma solvated lanthanoid(III) ions. The peak at ca. 3.5 Å corresponds to the Ln...C distance and is significantly longer in dma than dmf for all studied systems, which reflects a wider Ln–O–C angle in dma than in dmf. The respective angles were calculated from the obtained Ln–O and Ln...C distances as well as the average C–O bond length for coordinated dmf and dma from the Cambridge Structural Database.⁵⁷ The mean C–O bond distance is 1.244 Å for dmf and 1.250 Å for dma. The refined structure parameters and the Ln–O–C bond angles for all systems studied are given in Table 1.

EXAFS. The experimental EXAFS functions for the dmf, dma, and dmp solvated lanthanum(III) ion, the dmf and dma solvated gadolinium(III) ion, and the dma solvated lutetium(III) ion are shown in Figure 3. The corresponding Fourier transforms for the lanthanum(III) systems are shown in Figure 4. The fitted structure parameters for all listed systems are summarized in Table 2.

Significance of Structure Parameters from LAXS and EXAFS Measurements. The refined La–O bond distances from the LAXS and EXAFS measurements differ slightly, for example, 0.018 Å for the $[\text{La}(\text{dmf})_9]^{3+}$ complex, Tables 1 and 2. This is most likely due to the fact that the Ln–O bond distance distribution is slightly asymmetric giving the shorter distances in the distribution a larger contribution to the EXAFS function than longer ones. Consequently, an even larger difference is observed for the corresponding Ln...C distances. This bias toward shorter distances in a distribution is negligible in LAXS measurements. It should be noted that in the LAXS RDFs there are well-defined peaks attributed to the Ln...C distances, Figure 2. Conversely, the Ln...C interaction gives only a minor contribution to the EXAFS function and even though it may

Table 1. Interaction, Number of Distances (fixed), N , Mean Bond Distances, $d/\text{\AA}$, Temperature Coefficients, $b/\text{\AA}^2$, and the Calculated Bond Angle $\text{Ln}-\text{O}-\text{C}$ in Degrees, $\angle\text{Ln}-\text{O}-\text{C}/^\circ$, Obtained in the Refinements of the LAXS Data of the Solvated Lanthanum(III), Gadolinium(III) and Lutetium(III) Ions in dmf and dma Solution at Room Temperature

species ^a	interaction	N	d	b	$\angle\text{Ln}-\text{O}-\text{C}$
$\text{La}(\text{dmf})_9^{3+}$	La–O	9	2.553(7)	0.0121(6)	137(1)
	La \cdots C	9	3.566(4)	0.0159(4)	
$\text{La}(\text{dma})_8^{3+}$	La–O	8	2.523(5)	0.0110(8)	147(1)
	La \cdots C	8	3.637(9)	0.0119(2)	
$\text{Gd}(\text{dmf})_8^{3+}$	Gd–O	8	2.378(7)	0.0096(6)	139(1)
	Gd \cdots C	8	3.420(4)	0.0153(4)	
$\text{Gd}(\text{dma})_8^{3+}$	Gd–O	8	2.383(5)	0.0087(8)	154(2)
	Gd \cdots C	8	3.550(9)	0.0123(2)	
$\text{Lu}(\text{dmf})_8^{3+}$	Lu–O	8	2.303(7)	0.0041(6)	140(1)
	Lu \cdots C	8	3.349(4)	0.0160(4)	
$\text{Lu}(\text{dma})_7^{3+}$	Lu–O	7	2.260(5)	0.0085(8)	154(2)
	Lu \cdots C	7	3.427(9)	0.0148(2)	

^aStructures of the solvent molecules and the triflate ion have been kept constant in the refinements, see Table S5, Supporting Information.

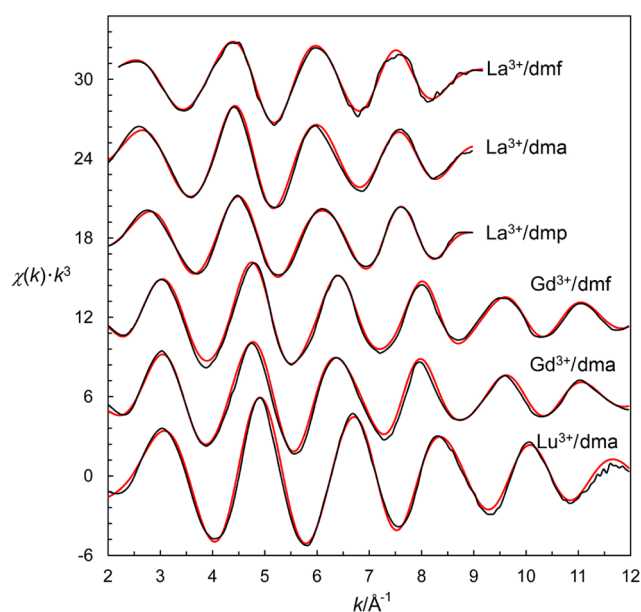


Figure 3. Experimental EXAFS data (black lines) fitted with a model formed by ab initio-calculated scattering paths (red lines), see Table 2. Offset: 6 (cumulative).

have a physical meaning, in most cases, the refined values are much more uncertain. This is an effect of the weighting of distances between the two techniques, where the contribution to the EXAFS function is strongly influenced by shorter distances while in LAXS measurements all distances are weighted equally.⁵⁸ For this reason, only the $\text{Ln}\cdots\text{C}$ distances obtained from LAXS data, and the corresponding calculated $\text{Ln}-\text{O}-\text{C}$ angles, will be used here.

Crystal Structure of 1. Octakis(*N,N*-dimethylacetamide)-lanthanum(III) triflate, **1**, crystallizes in space group $P2_1$ (No. 4), with two crystallographically independent lanthanum(III) ions, La1 and La2, Figure S6, Supporting Information. Each lanthanum(III) ion coordinates eight dma ligands in a square antiprismatic fashion, with a mean $\text{La}-\text{O}$ bond distance of

2.49(3) \AA , and with a mean $\text{La}-\text{O}-\text{C}$ bond angle of 150(12) $^\circ$. The crystal was of relatively low quality, with severe disorder and/or twinning, but a successful refinement was achieved through a large set of restraints from a measurement run under cold conditions (93 K). Five ligand positions were refined with dual positions for the dma backbone and left isotropic to keep the refinement stable. Selected bond distances and angles are listed in Table S4, Supporting Information.

DISCUSSION

The size of the amide oxygen. The crystal structures of homo- and heteroleptic lanthanoid(III) complexes with noncyclic amide ligands show that the mean $\text{Ln}-\text{O}$ bond distances are somewhat shorter compared to the mean of all reported structures with monodentate, neutral oxygen donors,⁵ Figure 5 (dashed lines) and Table S2, Supporting Information. The $\text{Ln}-\text{O}$ bond distance shortening is seen for all three CNs listed, $7 \leq \text{CN} \leq 9$, but it is only for eight-coordinate structures that valid comparisons can be made due to the limited amount of data for $\text{CN} = 7$ and 9. The slope of the eight-coordinate amide structures is almost parallel with the calculated $\text{CN} = 8$ slope of all structures, thus supporting the previously determined lanthanoid ionic radii.⁵ At the same time, this indicates that the amide oxygen radius is 1.32 \AA , ca. 0.02 \AA shorter than that of a water oxygen⁵⁹ likely due to the properties of the $\text{N}\cdots\text{C}\cdots\text{O}$ amide bond resonance.⁶⁰

Structure of Solvated Lanthanoid(III) Ions in Solution. *N,N*-Dimethylformamide. Based on the ionic radius of the lanthanum(III) ion in different configurations it can be concluded with high certainty that the CN of lanthanum(III) ion in dmf solution is centered around nine.⁵ The observed $\text{La}-\text{O}$ bond distances from both LAXS and EXAFS, Tables 1 and 2, are in the range with those reported for solids containing $[\text{La}(\text{dmf})_9]^{3+}$ complexes, Table S2, Supporting Information, giving a $\text{La}-\text{O}-\text{C}$ angle of 137(1) $^\circ$. Similarly, the LAXS results reveal that the gadolinium(III) ion is eight-coordinate in dmf with a refined $\text{Gd}-\text{O}$ distance of 2.378(7) \AA , Table 1. The corresponding distance obtained from EXAFS measurements is nearly identical, 2.376(6) \AA , Table 2. The obtained results fit well with both the revised eight-coordinate gadolinium(III) ionic radius⁵ and $\text{Gd}-\text{O}$ bond distances found in crystal structures of amide solvated gadolinium(III) ions, Table S2, Supporting Information. The $\text{Gd}\cdots\text{C}$ distance is 3.420(4) \AA , yielding a $\text{Gd}-\text{O}-\text{C}$ angle of 139(1) $^\circ$. Lastly, the $\text{Lu}-\text{O}$ bond distance of 2.303(7) \AA in dmf solution from the LAXS study suggests that the lutetium(III) ion is also eight-coordinate. This distance is almost identical to the mean $\text{Lu}-\text{O}$ bond distance reported for solid eight-coordinate dmf complexes.⁶¹ The refined $\text{Lu}\cdots\text{C}$ distance in dmf, 3.349(4) \AA , corresponds to a $\text{Lu}-\text{O}-\text{C}$ angle of 140(1) $^\circ$.

N,N-Dimethylacetamide. The result for the dma solvates is not as straightforward as the one for the dmf counterparts. The refined $\text{La}-\text{O}$ bond distance of the dma solvated lanthanum(III) ion obtained from LAXS is 2.523(5) \AA . The difference in bond length between the dmf and dma solvates, 0.030 \AA , is large enough to suggest different mean CNs of lanthanum(III) ion in dmf and dma. Data analysis lead to the conclusion that in dma solution there may be an equilibrium of eight- and nine-coordinate lanthanum(III) ions. The $\text{La}-\text{O}-\text{C}$ angle of 147(1) $^\circ$ in dma is 10 $^\circ$ larger than the one in the corresponding dmf solvate. The mean $\text{La}-\text{O}$ bond distance obtained by EXAFS, 2.505(6) \AA , falls in-between those expected for eight- and nine-coordination, respectively, Table S2. Furthermore, the

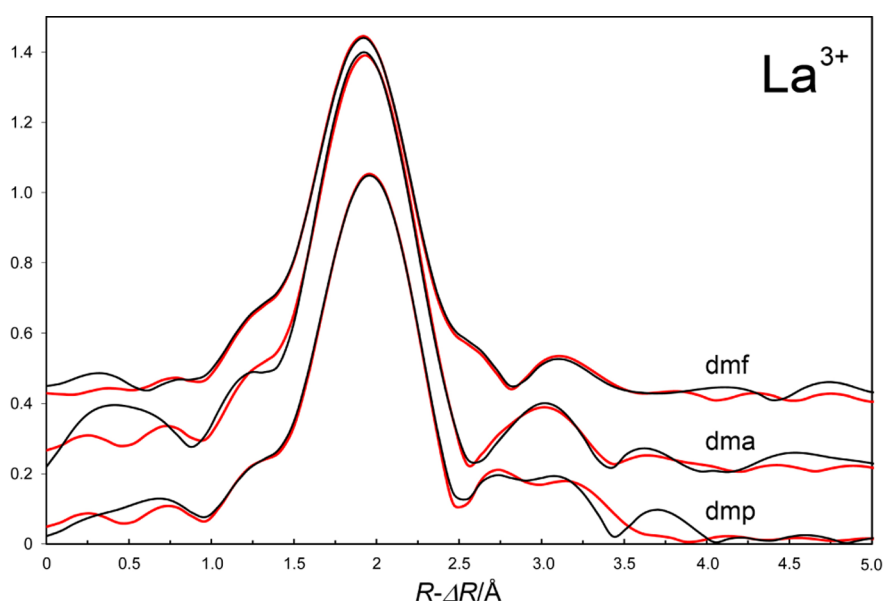


Figure 4. Fourier transformations (not phase corrected) of the EXAFS functions of dmf, dma, and dmp solvated lanthanum(III) ions, respectively, showing a clear difference in La–O bond distance for all three amide systems (black lines, experimental; red lines, model). Offset: 0.2 (cumulative).

Table 2. Scattering Path, Number of Distances (fixed), N , Mean Bond Distances, $R/\text{\AA}$, and Debye–Waller Coefficients, $\sigma^2/\text{\AA}^2$ in the Room Temperature EXAFS Studies of the Solvated Lanthanum(III), Gadolinium(III) and Lutetium(III) Ions in dmf, dma, and dmp Solution, Respectively^a

species	scattering path	N	R	σ^2
$\text{La}(\text{dmf})_9^{3+}$	La–O	9	2.535(6)	0.0102(8)
	La···C	9	3.487	0.0068
	La–O–C	18	3.637	0.0038
$\text{La}(\text{dma})_8^{3+}$	La–O	8	2.505(6)	0.0112(8)
	La···C	8	3.517	0.0206
	La–O–C	16	3.666	0.0084
$\text{La}(\text{dmp})_8^{3+}$	La–O	8	2.496(6)	0.0090(8)
	La···C	8	3.419	0.0064
	La–O–C	16	3.60	0.049
$\text{Gd}(\text{dmf})_8^{3+}$	Gd–O	8	2.376(6)	0.0068(8)
	Gd···C	8	3.614	0.0127
	Gd–O–C	16	3.83	0.0213
$\text{Gd}(\text{dma})_8^{3+}$	Gd–O	8	2.370(6)	0.0073(8)
	Gd···C	8	3.625	0.0110
	Gd–O–C	16	3.86	0.030
$\text{Lu}(\text{dma})_7^{3+}$	Lu–O	7	2.246(6)	0.0089(8)
	Lu···C	7	3.175	0.0092
	Lu–O–C	14	3.326	0.0165

^aError limits are given only for the refined values without restraints.

Debye–Waller coefficient in the EXAFS refinement for the lanthanum(III) dma solvate is fairly large supporting a wide bond distance distribution, which would also be indicative of an equilibrium between eight- and nine-coordinate lanthanum(III) ions. To some extent, this is supported by the shorter mean

La–O bond distance of the eight-coordinate $[\text{La}(\text{dma})_8]^{3+}$ complex in 1, 2.49(3) Å. The refined Gd–O bond distance from LAXS data is 2.383(5) Å, Table 1, and the corresponding distance obtained from the EXAFS measurement, 2.370(6) Å, Table 2, clearly shows that the dma solvated gadolinium(III) ion is eight-coordinate in solution. This is also supported by previously reported structures, Table S2, Supporting Information. The Gd···C distance is 3.550(9) Å, which yields a Gd–O–C angle of 154(2)°. The 0.043 Å difference in the Lu–O bond distances between dmf and dma solvates points to two different CNs for the lutetium(III) ion in these amide solvents. The refined Lu–O distance from the LAXS data of lutetium(III) in dma is 2.260(5) Å, Figure 4, while EXAFS measurements give a slightly shorter distance, 2.246(6) Å. The Lu–O distance for seven-coordinate reported earlier is 2.256 Å,⁵ strongly indicating that lutetium(III) ion is seven-coordinate in dma solution. The Lu···C distance in dma solution, 3.427(9) Å, results in a Lu–O–C angle of 154(2)°, compared to a 140(1)° angle in dmf. The angle is, however, more or less the same as in the eight-coordinate gadolinium(III) dma system which, based on the shorter Lu–O bond distance, suggests less crowding in the seven-coordinate lutetium(III) complex.

***N,N*-Dimethylpropionamide.** Due to experimental limitations, only EXAFS measurements were performed on the lanthanum(III) ion in dmp. The mean La–O bond distance of 2.496(6) Å falls between those expected for CN = 8 and 9, Table 2, close to that observed for 1. If the dmp solvate is a mixture of the two CNs, it is shifted more in the direction of CN = 8, which would be consistent with its increased steric requirements. An indication of this is seen in the Debye–Waller factor in the EXAFS refinement, which is larger than the gadolinium(III) dma solvate, but smaller than the lanthanum(III) dma solvate.

Relationship Between Solvate Structures and Standard Partial Molar Volumes. A thermodynamic perspective on the structural results for dmf and dma solvated lanthanoid(III) ions is presented in Table 3, where the standard partial molar volumes of the studied lanthanoid(III) triflates in dmf

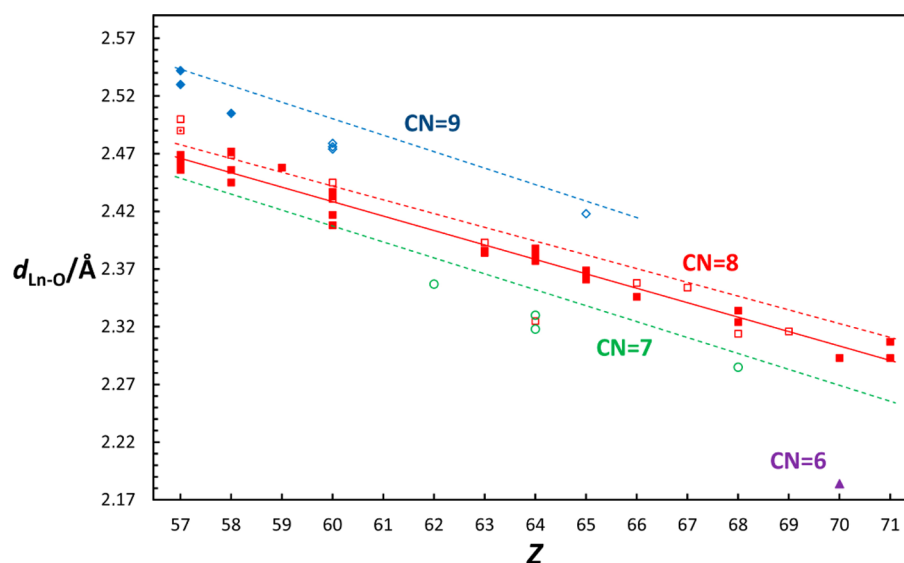


Figure 5. Distribution of mean Ln-O distances in noncyclic amides solvates (filled) and amide solvate/hydrates (empty) for $6 \leq \text{CN} \leq 9$, Table S2, Supporting Information. The expected bond distances for Ln-O bonds (dashed lines) are given for $7 \leq \text{CN} \leq 9$; see ref 5. The least-squares trendline for CN = 8 amide solvates (solid line) shows that mean amide Ln-O bond distances are shorter than for monodentate, neutral oxygen donor ligands in general. For full details, see ref 5.

Table 3. Standard Partial Molar Volumes of Lanthanum, Gadolinium and Lutetium Triflate in Water, dmf, and dma, as well as Their Ionic Contributions at 298 K^a

species	$V^\circ / \text{cm}^3 \text{mol}^{-1}$					
	H_2O^b	CN^c	dmf ^d	CN^e	dma ^d	CN^e
$\text{La}(\text{CF}_3\text{SO}_3)_3$	191.5(6)		163.6(3)		153.3(3)	
$\text{Gd}(\text{CF}_3\text{SO}_3)_3$	189.6(6)		163.2(3)		152.5(3)	
$\text{Lu}(\text{CF}_3\text{SO}_3)_3$	184.3 ^f		157.7(1)		152.5(2)	
La^{3+}	-39.2(3)	9	-49(5)	9	-63(5)	~8.5
Gd^{3+}	-40.5(3)	9	-50(5)	8	-64(5)	8
Lu^{3+}	-45.8(3)	8.2	-55(4)	8	-64(5)	7
CF_3SO_3^-	+76.7(5)		+71(1)		+72(2)	

^aThe estimated CNs for the amide solvated lanthanoid(III) ion, as determined in solution in this study and the previously reported aqueous system are listed for comparison. ^bReferences 25 and 28 (and references therein). ^cReference 7. ^dReference 45. ^eThis work. ^fCalculated.

and dma as well as their respective individual ionic contributions,⁴⁵ are listed together with the values for the same systems in aqueous solution.²⁸

A number of relationships between the structure of the solvated lanthanoid(III) ions and their standard partial molar volumes, V° , can be observed. The standard partial molar volumes decrease only marginally with the ionic radii of the lanthanoid(III) ions as long as the size of the solvent molecules is small enough to not interfere with each other upon coordination. This is true even when the CN changes from nine to eight, as seen in the very similar V° values for lanthanum(III) and gadolinium(III) ions in water and dmf, respectively. Coordination to a lanthanoid(III) ion may result in significant interference or crowding between solvent molecules which have a sufficiently large and bulky backbone structure. This is seen in the case for dma where the Ln-O-C angle is at least 10° larger than the dmf complexes which lack such crowding. We interpret this as a way for chemical systems to decrease ligand-ligand interference by making the required ligand volume smaller. For the dma systems, a decreasing ionic radius of the lanthanoid(III) ion is also accompanied with a decrease in CN, making the effect on the partial molar volume value insignificant as they cannot be packed any tighter. The

decrease in the volume of the GdO_n coordination core going from, for example, nine- to eight-coordination is ca. $4 \text{ cm}^3 \text{mol}^{-1}$, Table S6, Supporting Information. The effect of a decrease in CN is thus as large as the errors in the determination of standard partial molar volumes, implying that the effect of a coordination change may simply not be significant in the volumetric properties of a lanthanoid(III) ion. In addition, all solvents also have to make room for the triflate ion, but as waters form weak hydrogen bonds to the sulfonate end of the triflate ion, the expansion effect will be slightly smaller for water than aprotic solvents which solvate the triflate ion mainly through van der Waals forces. This shows that small solvent molecules and larger space-demanding ones, upon coordination, influence the standard partial molar volume in different ways. With small solvent molecules, such as water and dmf, the solvated metal ions will have approximately the same V° value as long as the configuration and ionic radii are not changing too much. Conversely, space-demanding solvent molecules, which interfere with one another in the solvate complex structure, bring about a decrease in CN with decreasing ionic radii of the lanthanoid(III) ion while maintaining a (minimum) V° value, as observed for the dma systems. One explanation for this is that more space-demanding

molecule ought to shield the ionic charge to a larger extent, making the electrostriction effect smaller or possibly negligible. However, such comparisons between aqueous and nonaqueous solvents are more difficult to make as hydrated lanthanoid(III) ions undergo volume changes in multiple hydration shells. Nevertheless, the V° values decrease with increasing size and spatial demands of the solvent molecule, Table 3.

CONCLUSIONS

The structures of the N,N -dimethylformamide (dmf), N,N -dimethylacetamide (dma), and N,N -dimethylpropionamide (dmp) solvated lanthanum(III), gadolinium(III) and lutetium(III) have been determined in solution by means of EXAFS and LAXS. The coordination number is affected by the increasing spatial demand upon coordination in the order $\text{dmf} < \text{dma} < \text{dmp}$ due to increasing volume of the backbone structure. The coordination number of lanthanum(III) seems to decrease from nine in dmf to close to eight in dmp, indicating an equilibrium between coordination number eight and nine in dma and dmp. Solid $[\text{La}(\text{dma})_8](\text{CF}_3\text{SO}_3)_3$ is eight-coordinate in square antiprismatic fashion with a slightly shorter mean La–O bond distance than in solution supporting equilibrium of two coordination numbers. The gadolinium(III) ion is eight-coordinate in both dmf and dma, while the lutetium(III) is eight- and seven-coordinate in dmf and dma, respectively. One aim of this study was to combine results from the structural study with volumetric data for these systems. The lanthanoid contraction and differences in spatial requirements of the amide backbone validate the observed decrease in coordination number, which is indeed supported by both the structural and volumetric data, though either set of data by itself does not reveal all the changes these different systems undergo. However, taken together, and in combination with previous studies in the solid state, these analyses contribute to a more complete understanding of lanthanoid(III) amide systems. This ultimately shows the risk of relying on a single approach when attempting to interpret the underlying meaning of data and the importance of combining both structural and thermodynamic measurements even when dealing with carefully selected systems.

ASSOCIATED CONTENT

Supporting Information

Crystallographic information file for **1**, additional LAXS RDFs and their reduced intensity functions (Figures S1–S5), a representation of the positional disorder in **1** (Figure S6), selected physicochemical properties of dmf, dma, and dmp (Table S1), previously reported noncyclic amide structures (Table S2) and relevant structure parameters/data (Tables S3–S6). This material is available free of charge via the Internet at <http://pubs.acs.org>.

AUTHOR INFORMATION

Corresponding Author

*E-mail: daniel.lundberg@slu.se.

Notes

The authors declare no competing financial interest.

[§]née Placzek.

ACKNOWLEDGMENTS

The Swedish Institute is acknowledged for supporting Anna Fuchs through the Visby Program during her stay in Sweden.

The support to Ingmar Persson for the solution chemistry research from the Swedish Research Council is gratefully acknowledged. Portions of this research were carried out at the Stanford Synchrotron Radiation Lightsource (SSRL), and the MAX-lab synchrotron radiation source at Lund University, Sweden, which are acknowledged for the allocation of beam time and laboratory facilities. Portions of this research were carried out at the Stanford Synchrotron Radiation Lightsource, a Directorate of SLAC National Accelerator Laboratory and an Office of Science User Facility operated for the U.S. Department of Energy Office of Science by Stanford University. The SSRL Structural Molecular Biology Program is supported by the DOE Office of Biological and Environmental Research, and by the National Institutes of Health, National Center for Research Resources, Biomedical Technology Program (P41RR001209). Portions of this research were carried out at beamline I811, MAX-lab synchrotron radiation source, Lund University, Sweden. Funding for the beamline I811 project was provided by the Swedish Research Council and The Knut and Alice Wallenbergs Foundation.

REFERENCES

- (1) Abbasi, A.; Lindqvist-Reis, P.; Eriksson, L.; Sandström, D.; Lidin, S.; Persson, I.; Sandström, M. Highly Hydrated Cations: Deficiency, Mobility, and Coordination of Water in Crystalline Nonhydrated Scandium(III), Yttrium(III), and Lanthanoid(III) Trifluoromethanesulfonates. *Chem.—Eur. J.* **2005**, *11*, 4065–4077.
- (2) D'Angelo, P.; De Panfilis, S.; Filipponi, A.; Persson, I. High-Energy X-ray Absorption Spectroscopy: A New Tool for Structural Investigations of Lanthanoids and Third-Row Transition Elements. *Chem.—Eur. J.* **2008**, *14*, 3045–3055.
- (3) D'Angelo, P.; Zitolo, A.; Migliorati, V.; Mancini, G.; Persson, I.; Chillemi, G. Structural Investigation of Lanthanoid Coordination: a Combined XANES and Molecular Dynamics Study. *Inorg. Chem.* **2009**, *48*, 10239–10248.
- (4) D'Angelo, P.; Zitolo, A.; Migliorati, V.; Persson, I. Analysis of the Detailed Configuration of Hydrated Lanthanoid(III) Ions in Aqueous Solution and Crystalline Salts by Using K- and L₃-Edge XANES Spectroscopy. *Chem.—Eur. J.* **2010**, *16*, 684–692.
- (5) Lundberg, D.; Persson, I.; Eriksson, L.; D'Angelo, P.; De Panfilis, S. Structural Study of the N,N' -Dimethylpropyleneurea Solvated Lanthanoid(III) Ions in Solution and Solid State with an Analysis of the Ionic Radii of Lanthanoid(III) Ions. *Inorg. Chem.* **2010**, *49*, 4420–4432.
- (6) Näslund, J.; Lindqvist-Reis, P.; Persson, I.; Sandström, M. Steric Effects Control the Structure of the Solvated Lanthanum(III) Ion in Aqueous, Dimethyl Sulfoxide, and N,N' -Dimethylpropyleneurea Solution. An EXAFS and Large-Angle X-ray Scattering Study. *Inorg. Chem.* **2000**, *39*, 4006–4011.
- (7) Persson, I.; D'Angelo, P.; De Panfilis, S.; Sandström, M.; Eriksson, L. Hydration of Lanthanoid(III) Ions in Aqueous Solution and Crystalline Hydrates Studied by EXAFS Spectroscopy and Crystallography: the Myth of the “Gadolinium Break”. *Chem.—Eur. J.* **2008**, *14*, 3056–3066.
- (8) Abbasi, A.; Risberg, E. D.; Eriksson, L.; Mink, J.; Persson, I.; Sandström, M.; Sidorov, Y. V.; Skripkin, M. Y.; Ullström, A.-S. Crystallographic and Vibrational Spectroscopic Studies of Octakis-(dmso)lanthanoid(III) Iodides. *Inorg. Chem.* **2007**, *46*, 7731–7741.
- (9) Persson, I.; Risberg, E. D.; D'Angelo, P.; De Panfilis, S.; Sandström, M.; Abbasi, A. X-ray Absorption Fine Structure Spectroscopic Studies of Octakis(dmso)lanthanoid(III) Complexes in Solution and in the Solid Iodides. *Inorg. Chem.* **2007**, *46*, 7742–7748.
- (10) Shannon, R. D. Revised Effective Ionic Radii and Systematic Studies of Interatomic Distances in Halides and Chalcogenides. *Acta Crystallogr., Sect. A* **1976**, *32*, 751–767.

- (11) Sandström, M.; Persson, I.; Persson, P. A Study of Solvent Electron-Pair Donor Ability and Lewis Basicity Scales. *Acta Chem. Scand.* **1990**, *44*, 653–675.
- (12) Asada, M.; Mitsugi, T.; Fujii, K.; Kanzaki, R.; Umebayashi, Y.; Ishiguro, S.-i. Vibrational Spectroscopy and Molecular Orbital Calculations of *N,N*-Dimethylacrylamide and *N,N*-Dimethylpropionamide - Conformational Equilibrium in the Liquid State. *J. Mol. Liq.* **2007**, *136*, 138–146.
- (13) Murugan, R.; Mohan, S. Vibrational-Spectra and Normal-Coordinate Analysis of *N,N*-Dimethylpropionamide. *Spectrochim. Acta, Part A* **1995**, *51*, 735–735.
- (14) Umebayashi, Y.; Matsumoto, K.; Mune, Y.; Zhang, Y.; Ishiguro, S.-i. Conformational Equilibria of solvent *N,N*-Dimethylpropionamide in the Bulk and in the Coordination Sphere of the Manganese(II) Ion. *Phys. Chem. Chem. Phys.* **2003**, *5*, 2552–2556.
- (15) Di Bernardo, P.; Melchior, A.; Tolazzi, M.; Zanonato, P. L. Thermodynamics of Lanthanide(III) Complexation in Non-Aqueous Solvents. *Coord. Chem. Rev.* **2012**, *256*, 328–351.
- (16) Di Bernardo, P.; Melchior, A.; Tolazzi, M.; Zanonato, P. L. Corrigendum to “Thermodynamics of Lanthanide(III) Complexation in Non Aqueous Solvents” [*Coord. Chem. Rev.* 256 (1) (2011) 328–351]. *Coord. Chem. Rev.* **2012**, *256*, 1279–1280.
- (17) Hefter, G.; Marcus, Y. A Critical Review of Methods for Obtaining Ionic Volumes in Solution. *J. Solution Chem.* **1997**, *26*, 249–266.
- (18) Marcus, Y. Effects of Ions on the Structure of Water: Structure Making and Breaking. *Chem. Rev.* **2009**, *109*, 1346–1370.
- (19) Marcus, Y.; Hefter, G. Standard Partial Molar Volumes of Electrolytes and Ions in Nonaqueous Solvents. *Chem. Rev.* **2004**, *104*, 3405–3452.
- (20) Placzek, A.; Grzybkowski, W.; Hefter, G. Molar Volumes and Heat Capacities of Electrolytes and Ions in *N,N*-Dimethylformamide. *J. Phys. Chem. B* **2008**, *112*, 12366–12373.
- (21) Hepler, L. G. Partial Molal Volumes of Aqueous Ions. *J. Phys. Chem.* **1957**, *61*, 1426–1429.
- (22) Marcus, Y. Electrostriction, Ion Solvation, and Solvent Release on Ion Pairing. *J. Phys. Chem. B* **2005**, *109*, 18541–18549.
- (23) Erickson, K. M.; Hakin, A. W.; Jones, S. N.; Liu, J. L.; Zahir, S. N. Thermodynamics of Selected Aqueous Rare-Earth Elements Containing Triflate Salts at T=(288.15, 298.15, 313.15 and 328.15) K and P=0.1 MPa. *J. Solution Chem.* **2007**, *36*, 1679–1726.
- (24) Xiao, C. B.; Tremaine, P. R. Apparent Molar Heat Capacities and Volumes of LaCl_3 (aq), $\text{La}(\text{ClO}_4)_3$ (aq), and $\text{Gd}(\text{ClO}_4)_3$ (aq) Between the Temperatures 283 and 338 K. *J. Chem. Thermodyn.* **1996**, *28*, 43–66.
- (25) Xiao, C. B.; Tremaine, P. R.; Simonson, J. M. Apparent Molar Volumes of $\text{La}(\text{CF}_3\text{SO}_3)_3$ (aq) and $\text{Gd}(\text{CF}_3\text{SO}_3)_3$ (aq) at 278 K, 298 K, and 318 K at Pressures to 30.0 MPa. *J. Chem. Eng. Data* **1996**, *41*, 1075–1078.
- (26) Hakin, A. W.; Liu, J. L.; Erickson, K.; Munoz, J. V.; Rard, J. A. Apparent Molar Volumes and Apparent Molar Heat Capacities of $\text{Pr}(\text{NO}_3)_3$ (aq), $\text{Gd}(\text{NO}_3)_3$ (aq), $\text{Ho}(\text{NO}_3)_3$ (aq), and $\text{Y}(\text{NO}_3)_3$ (aq) at T = (288.15, 298.15, 313.15, and 328.15) K and P = 0.1 MPa. *J. Chem. Thermodyn.* **2005**, *37*, 153–167.
- (27) Buz'ko, V. Y.; Sukhno, I. V.; Panyushkin, V. T. Physical and Thermodynamic Characteristics of Aqueous Solutions of Rare-Earth Salts. *Russ. J. Inorg. Chem.* **2004**, *49*, 1613–1616.
- (28) Marriott, R. A.; Hakin, A. W.; Rard, J. A. Apparent Molar Heat Capacities and Apparent Molar Volumes of $\text{Y}_2(\text{SO}_4)_3$ (aq), $\text{La}_2(\text{SO}_4)_3$ (aq), $\text{Pr}_2(\text{SO}_4)_3$ (aq), $\text{Nd}_2(\text{SO}_4)_3$ (aq), $\text{Eu}_2(\text{SO}_4)_3$ (aq), $\text{Dy}_2(\text{SO}_4)_3$ (aq), $\text{Ho}_2(\text{SO}_4)_3$ (aq), and $\text{Lu}_2(\text{SO}_4)_3$ (aq) at T=298.15 K and P=0.1 MPa. *J. Chem. Thermodyn.* **2001**, *33*, 643–687.
- (29) Warminska, D.; Wawer, J. Apparent Molar Volumes and Compressibilities of Lanthanum, Gadolinium and Lutetium Trifluoromethanesulfonates in Dimethylsulfoxide. *J. Chem. Thermodyn.* **2012**, *55*, 79–84.
- (30) Wawer, J.; Warminska, D.; Grzybkowski, W. Solvation of Multivalent Cations in Methanol - Apparent Molar Volumes, Expansibilities, and Isentropic Compressibilities. *J. Chem. Thermodyn.* **2011**, *43*, 1731–1737.
- (31) Ishiguro, S.-i.; Umebayashi, Y.; Kato, K.; Takahashi, R.; Ozutsumi, K. Strong and Weak Solvation Steric Effects on Lanthanoid(III) Ions in *N,N*-Dimethylformamide/*N,N*-Dimethylacetamide Mixtures. *J. Chem. Soc., Faraday Trans.* **1998**, *94*, 3607–3612.
- (32) Ishiguro, S.-i.; Umebayashi, Y.; Komiya, M. Thermodynamic and Structural Aspects on the Solvation Steric Effect of Lanthanide(III)—Dependence on the Ionic Size. *Coord. Chem. Rev.* **2002**, *226*, 103–111.
- (33) Umebayashi, Y.; Matsumoto, K.; Mekata, I.; Ishiguro, S.-i. Solvation Structure of Lanthanide(III) Ions in Solvent Mixtures of *N,N*-Dimethylformamide and *N,N*-Dimethylacetamide Studied by Titration Raman Spectroscopy. *Phys. Chem. Chem. Phys.* **2002**, *4*, 5599–5605.
- (34) Ishiguro, S.-i. Thermodynamic and Structural Aspects on Solvation Steric Effect in Nonaqueous Solution. *Bull. Chem. Soc. Jpn.* **1997**, *70*, 1465–1477.
- (35) Ishiguro, S.-i.; Umebayashi, Y.; Kanzaki, R. Characterization of Metal Ions in Coordinating Solvent Mixtures by Means of Raman Spectroscopy. *Anal. Sci.* **2004**, *20*, 415–421.
- (36) Ishiguro, S.-i.; Kato, K.; Takahashi, R.; Nakasone, S. Non-aqueous Solution Chemistry of Lanthanide(III) Ions. *Rare Earths* **1995**, *27*, 61–77.
- (37) Komiya, M.; Nishikido, Y.; Umebayashi, Y.; Ishiguro, S.-i. Formation Thermodynamics of Binary and Ternary Lanthanide(III) Complexes with 1,10-Phenanthroline and Chloride in *N,N*-Dimethylformamide. *J. Solution Chem.* **2002**, *31*, 931–946.
- (38) Pisaniello, D. L.; Helm, L.; Zbinden, D.; Merbach, A. E. A Demonstrated Example of Competing D and ID Mechanisms for Dimethylformamide Exchange on the Octakis(dimethylformamide)-Erbium(III) Ion. *Helv. Chim. Acta* **1983**, *66*, 1872–1875.
- (39) Pisaniello, D. L.; Merbach, A. E. Variable Temperature Multi-Nuclear NMR - Investigation of Dimethylformamide Exchange on the Octakis(*N,N*-Dimethylformamide)-Thulium(III) Ion. *Helv. Chim. Acta* **1982**, *65*, 573–581.
- (40) Pisaniello, D. L.; Nichols, P. J.; Ducommun, Y.; Merbach, A. E. Spectrophotometric and Nuclear Magnetic-Resonance Study of Temperature-Induced and Pressure-Induced Changes in the Intimate Solvation of Neodymium(III) in *N,N*-Dimethylformamide and Trimethylphosphate. *Helv. Chim. Acta* **1982**, *65*, 1025–1028.
- (41) Pisaniello, D. L.; Helm, L.; Meier, P.; Merbach, A. E. Variable Pressure and Temperature Nuclear Magnetic Resonance and Visible Spectrophotometric Studies of Lanthanide Ions in Dimethylformamide: Solvation and Solvent Exchange Dynamics. *J. Am. Chem. Soc.* **1983**, *105*, 4528–4536.
- (42) Buz'ko, V. Y.; Kashaev, D. V.; Sukhno, I. V.; Panyushkin, V. T. ^{17}O NMR Study of the Solvation State of Gd^{3+} Ions in *N,N*-Dimethylformamide. *Russ. J. Phys. Chem. A* **2010**, *84*, 1252–1254.
- (43) Grigor'ev, M. S.; Shirokova, I. B.; Fedoseev, A. M.; Den Auwer, C. Crystal Structure of Hexakis(*N,N*-Dimethylacetamide)ytterbium(III) Dodecawolframophosphate $[\text{Yb}(\text{DMAA})_6]\text{PW}_{12}\text{O}_{40}$. *Cryst. Rep.* **2003**, *48*, 638–640.
- (44) Moeller, T.; Vicentini, G. Observations on Rare Earths 0.77. Anhydrous *N,N*-Dimethylacetamide Adducts of Tri-Positive Perchlorates. *J. Inorg. Nucl. Chem.* **1965**, *27*, 1477–1482.
- (45) Warminska, D.; Fuchs, A.; Lundberg, D. Apparent Molar Volumes and Compressibilities of Lanthanum, Gadolinium, Lutetium and Sodium Trifluoromethanesulfonates in *N,N*-Dimethylformamide and *N,N*-Dimethylacetamide. *J. Chem. Thermodyn.* **2013**, *58*, 46–54.
- (46) Johansson, G. An X-Ray Investigation of the Structure of the Hg_2^{2+} Ion in Solution. *Acta Chem. Scand.* **1966**, *20*, 553–562.
- (47) Johansson, G. An X-Ray Investigation of the Hydrolysis Products of Mercury(II) in Solution. *Acta Chem. Scand.* **1971**, *25*, 2787–2798.
- (48) Johansson, G.; Sandström, M. Computer-Programs for Analysis of Data on X-Ray-Diffraction by Liquids. *Chem. Scr.* **1973**, *4*, 195–198.
- (49) Stålhandske, C. M. V.; Persson, I.; Sandström, M.; Kamieńska-Piotrowicz, E. Crystal Structure of *N,N*-dimethylthioformamide

Solvates of the Divalent Group 12 Ions with Linear Coordination Geometry for Mercury(II), Tetrahedral for Zinc(II), and Octahedral for Cadmium(II). *Inorg. Chem.* **1997**, *36*, 3167–3173.

(50) *International Tables for X-ray Crystallography*; Kynoch Press: Birmingham, U.K., 1974.

(51) Cromer, D. T. Compton Scattering Factors for Aspherical Free Atoms. *J. Chem. Phys.* **1969**, *50*, 4857–4859.

(52) Levy, H. A.; Danford, M. D.; Narten, A. H. *Data Collection and Evaluation with an X-ray Diffractometer Designed for the Study of Liquid Structure*; Oak Ridge National Laboratory: Oak Ridge, TN, 1966.

(53) Molund, M.; Persson, I. STEPLR - a Program for Refinements of Data on X-Ray-Scattering by Liquids. *Chem. Scr.* **1985**, *25*, 197–197.

(54) Robinson, J. W. *Handbook of Spectroscopy*; CRC Press: Boca Raton, FL, 1991.

(55) George, G. N.; Pickering, I. J. EXAFSPAK - A Suite of Computer Programs for Analysis of X-ray Absorption Spectra; SSRL: Stanford, CA, 1993.

(56) Sheldrick, G. M. A Short History of SHELX. *Acta Crystallogr., Sect. A* **2008**, *64*, 112–122.

(57) Allen, F. H. The Cambridge Structural Database: a Quarter of a Million Crystal Structures and Rising. *Acta Crystallogr. Sect. B* **2002**, *58*, 380–388.

(58) Persson, I.; Sandström, M.; Yokoyama, H.; Chaudhry, M. Structure of the Solvated Strontium and Barium Ions in Aqueous, Dimethyl-Sulfoxide and Pyridine Solution, and Crystal-Structure of Strontium and Barium Hydroxide Octahydrate. *Z. Naturforsch., A* **1995**, *50*, 21–37.

(59) Beattie, J. K.; Best, S. P.; Skelton, B. W.; White, A. H. Structural Studies on the Caesium Alums, $\text{CsM}^{\text{III}}[\text{SO}_4]_2 \cdot 12\text{H}_2\text{O}$. *J. Chem. Soc., Dalton Trans.* **1981**, 2105–2111.

(60) Kemnitz, C. R.; Loewen, M. J. "Amide Resonance" Correlates with a Breadth of C-N Rotation Barriers. *J. Am. Chem. Soc.* **2007**, *129*, 2521–2528.

(61) Yarovoi, S. S.; Mironov, Y. V.; Solodovnikov, S. F.; Solodovnikova, Z. A.; Naumov, D. Y.; Fedorov, V. E. A Morphotropic Series of the Cluster Complexes $[\text{Ln}(\text{DMF})_8][\text{Re}_6\text{Q}_7\text{Br}_7]$ (Q = S, Se): Synthesis, Structure, and Thermal Transformations. *Russ. J. Coord. Chem.* **2006**, *32*, 712–722.